Supplemental text

Kinetic model

Nomenclature

DNA: DNA encoding aptazyme and GFP gene,

F: free full-length mRNA,

L: ligand (TPP),

FL: ligand-bound form of the full-length mRNA,

C: cleaved mRNA,

Protein: GFP protein

k_{Txn}: transcription rate,

k_{Deg1}: degradation rate of the full-length mRNA,

k_{Deg2}: degradation rate of the cleaved mRNA,

k_{Cle1}: cleavage rate of the ligand-bound form of the full-length RNA,

k_{Cle2}: cleavage ratio of the ligand-unbound form of the full-length RNA,

k_{on}: ligand association rate,

k_{off}: ligand dissociation rate,

k_{Pro1}: translation rate from the cleaved mRNA,

k_{Pro2}: translation rate from the full-length mRNA

Derivation of equations

Based on the scheme shown in Fig. 1b, deviations of each component were derived as follows,

$$\frac{d[F]}{dt} = k_{Txn}[DNA] - k_{Cle2}[F] - k_{on}[F][L] + k_{off}[FL] - k_{Deg1}[F] \quad \text{eq. 1}$$

$$\frac{d[FL]}{dt} = k_{on}[F][L] - k_{off}[FL] - k_{Cle1}[FL] - k_{Deg1}[FL] \quad \text{eq. 2}$$

$$\frac{d[C]}{dt} = k_{Cle1}[FL] + k_{Cle2}[F] - k_{Deg2}[C] \quad \text{eq. 3}$$

$$\frac{d[Protein]}{dt} = k_{Pro1}[C] + k_{Pro2}([F] + [FL]) \quad \text{eq. 4}$$

$$\frac{d[RNA_{degraded}]}{dt} = k_{Deg1}[F] + k_{Deg1}[FL] + k_{Deg2}[C] \quad , \quad \text{eq. 5}$$

where [RNA degraded] represents total degraded RNA concentration. These equations include components that are difficult to measure experimentally, such as the free full-length RNA (F) and the ligand-bound full-length RNA (FL). Therefore, we attempted to convert these equations into forms containing the measurable component, the total full-length RNA (F + FL).

We assumed that the association and dissociation between ligand and full-length RNA come to equilibrium immediately, yielding

$\frac{[F][L]}{[FL]} = K_d$, where $K_d = \frac{k_{off}}{k_{on}}$.

This equation was converted to

$[FL] = \frac{[F_{Total}][L]}{K_d+[L]}$,

where $[F_{Total}] = [F] + [FL]$. eq, 6

As the ligand (TPP) was present in excess over the full-length RNA under our experimental conditions, the free ligand concentration ([L]) was almost equal to the total ligand concentration ($[L_{Total}]$), yielding

$[FL] = \frac{[F_{Total}][L_{Total}]}{K_d+[L_{Total}]}$. eq. 7

Deviation of the total full-length RNA is obtained by adding eq. 1 and eq. 2, resulting in,

$\frac{d[F_{Total}]}{dt} = k_{Txn}[DNA] - k_{Cle2}[F] - k_{Cle1}[FL] - k_{Deg1}[F_{Total}]$.

This equation was substituted with eq. 6 and eq. 7 to yield

$\frac{d[F_{Total}]}{dt} = k_{Txn}[DNA] - k_{Cle2}[F_{Total}] + (k_{Cle2} - k_{Cle1})\frac{[F_{Total}][L_{Total}]}{K_d+[L_{Total}]} - k_{Deg1}[F_{Total}]$.

Here, we assumed that k_{Cle1} (self-cleavage activity of ligand-bound form) is much larger than k_{Cle2} (self-cleavage activity of ligand-unbound form),

that is $k_{Cle1} >> k_{Cle2}$. eq. 8

This assumption is reasonable because aptazymes were originally designed to have higher ribozyme activity in ligand-bound form than in ligand-unbound form. Therefore, this equation can be converted to

$\frac{d[F_{Total}]}{dt} = k_{Txn}[DNA] - (k_{Cle2} + k_{Deg1} + \frac{k_{Cle1}[L_{Total}]}{K_d+[L_{Total}]})[F_{Total}]$. eq. 9

Using eq. 6, 7, and 8, eq. 3 can also be converted to

$$\frac{d[C]}{dt} = (\frac{k_{Cle1}[L_{Total}]}{K_d+[L_{Total}]} + k_{Cle2})[F_{Total}] - k_{Deg2}[C].$$ eq. 10

In the same way, eq. 4 and eq. 5 can be converted to

$$\frac{d[Protein]}{dt} = k_{Pro1}[C] + k_{Pro2}[F_{Total}]$$ and eq. 11

$$\frac{d[RNA_{degraded}]}{dt} = k_{Deg1}[F_{Total}] + k_{Deg2}[C]$$, respectively. eq. 12

Eq. 9 and 10 are solved analytically to yield

$$[F_{Total}] = \frac{k_{Txn}[DNA]}{\alpha}(1 - e^{-\alpha t}),$$ eq. 13

where $\alpha = k_{Cle2} + k_{Deg1} + \frac{k_{Cle1}[L_{Total}]}{K_d+[L_{Total}]}$, . eq. 14

and $[C] = \frac{k_{Txn}[DNA](\alpha-k_{Deg1})}{\alpha-k_{Deg2}}\left(\frac{1-e^{-k_{Deg2}t}}{k_{Deg2}} - \frac{1-e^{-\alpha t}}{\alpha}\right)$. eq.15

The total RNA concentration, which includes the full-length RNA, cleaved RNA, and all of the degraded RNA, is represented as

$$[RNA_{Total}] = [F_{Total}] + [C] + [RNA_{degraded}].$$

According to eq. 9, 10, and 12, the deviation of the total RNA concentration is given as

$$\frac{d[mRNA_{Total}]}{dt} = k_{Txn}[DNA].$$

Integrating this equation yields

$$[mRNA_{Total}] = k_{Txn}[DNA]t.$$ eq. 16

Eq.11 is further converted to

$$\frac{d[Protein]}{dt}/[F_{Total}] = k_{Pro1}[C]/[F_{Total}] + k_{Pro2}. \qquad \text{eq. 17}$$

S/N ratio at steady-state

The S/N ratio is defined as the ratio of the protein concentration in the presence of excess ligand to that in the absence of ligand. The deviation of protein concentration is given by eq. 11, 13, and 15 as

$$\frac{d[Protein]}{dt} = k_{Pro1}\frac{k_{Txn}[DNA](\alpha - k_{Deg1})}{\alpha - k_{Deg2}}\left(\frac{1-e^{-k_{Deg2}t}}{k_{Deg2}} - \frac{1-e^{-\alpha t}}{\alpha}\right) + k_{Pro2}\frac{k_{Txn}[DNA]}{\alpha}(1 - e^{-\alpha t}).$$

Integration of this equation gives

$$[Protein] =$$

$$k_{Pro1}\frac{k_{Txn}[DNA](\alpha - k_{Deg1})}{\alpha - k_{Deg2}}\left(\frac{\mathrm{t}}{k_{Deg2}} + \frac{e^{-k_{Deg2}t}}{{k_{Deg2}}^2} - \frac{\mathrm{t}}{\alpha} - \frac{e^{-\alpha t}}{\alpha^2} - \frac{1}{{k_{Deg2}}^2} + \frac{1}{\alpha^2}\right) + k_{Pro2}k_{Txn}[DNA]\left(\frac{\mathrm{t}}{\alpha} + \frac{e^{-\alpha t}}{\alpha^2} - \frac{1}{\alpha^2}\right). \qquad \text{eq.18}$$

The first and second terms represent translation from the cleaved RNA (i.e., Ligand-dependent route + Ligand-independent route 1 in Fig. 1c) and translation from the full-length RNA (i.e., Ligand-independent route 2), respectively.

First, we attempted to calculate Signal, the protein expression in the presence of excess ligand. For Signal, the second term is neglected because on-switch aptazymes are

usually designed to express protein from cleaved RNA, not from full-length RNA, in the presence of excess ligand. From eq. 8, 14, and the assumption that ligand concentration is present in excess over K_d value (i.e., [L] >> K_d), we obtained Signal expression as

$$[Protein]_{Signal} = k_{Pro1}\frac{k_{Txn}[DNA](\alpha - k_{Deg1})}{\alpha - k_{Deg2}}\left(\frac{\mathrm{t}}{k_{Deg2}} + \frac{e^{-k_{Deg2}t}}{{k_{Deg2}}^2} - \frac{\mathrm{t}}{k_{Deg1}+k_{Cle1}} - \frac{e^{-(k_{Deg1}+k_{Cle1})t}}{(k_{Deg1}+k_{Cle1})^2} - \frac{1}{{k_{Deg2}}^2} + \frac{1}{(k_{Deg1}+k_{Cle1})^2}\right).$$

Second, we attempted to calculate Noise, the protein expression in the absence of ligand. Noise can be given by different formula depending on the route of production as follows.

Case 1: The protein is translated from the cleaved RNA produced without ligand binding, designated as "Ligand-independent route 1" in Fig. 1c. The second term of eq. 18 is negligible. From eq. 14, we obtained the Noise expression as

$$[\mathrm{Protein}]^{route1}_{Noise} = k_{Pro1}\frac{k_{Txn}[DNA](\alpha - k_{Deg1})}{\alpha - k_{Deg2}}\left(\frac{\mathrm{t}}{k_{Deg2}} + \frac{e^{-k_{Deg2}t}}{{k_{Deg2}}^2} - \frac{\mathrm{t}}{k_{Cle2}+k_{Deg1}} - \frac{e^{-(k_{Cle2}+k_{Deg1})t}}{(k_{Cle2}+k_{Deg1})^2} - \frac{1}{{k_{Deg2}}^2} + \frac{1}{(k_{Cle2}+k_{Deg1})^2}\right).$$

The S/N ratio in this case is given by dividing eq. 18 by this equation, yielding

$$\frac{\mathrm{S}}{\mathrm{N}}^{route1} = \frac{\left(\frac{\mathrm{t}}{k_{Deg2}} + \frac{e^{-k_{Deg2}t}}{{k_{Deg2}}^2} - \frac{\mathrm{t}}{k_{Deg1}+k_{Cle1}} - \frac{e^{-(k_{Deg1}+k_{Cle1})t}}{(k_{Deg1}+k_{Cle1})^2} - \frac{1}{{k_{Deg2}}^2} + \frac{1}{(k_{Deg1}+k_{Cle1})^2}\right)}{\left(\frac{\mathrm{t}}{k_{Deg2}} + \frac{e^{-k_{Deg2}t}}{{k_{Deg2}}^2} - \frac{\mathrm{t}}{k_{Cle2}+k_{Deg1}} - \frac{e^{-\left(k_{Cle2}+k_{Deg1}\right)t}}{\left(k_{Cle2}+k_{Deg1}\right)^2} - \frac{1}{{k_{Deg2}}^2} + \frac{1}{\left(k_{Cle2}+k_{Deg1}\right)^2}\right)}.$$

At steady-state (i.e., after infinite time), both the terms that are constant and that

contain an exponential function of $-t$ are negligible compared to the terms with first order of t. Therefore, S/N ratio at steady-state in this case is given as

$$\mathrm{S/N}^{route1} = \frac{(k_{Cle1}+k_{Deg1}-k_{Deg2})(k_{Cle2}+k_{Deg1})}{(k_{Cle2}+k_{Deg1}-k_{Deg2})(k_{Cle1}+k_{Deg1})}.$$

Case 2: The protein is expressed by leaky translation from the full-length RNA designated as "Ligand-independent route 2" in Fig. 1c. The first term of eq. 18 is negligible, and from eq. 14, we obtained Noise expression as

$$[\mathrm{Protein}]_{Noise}^{route2} = k_{Pro2}k_{Txn}[DNA]\left(\frac{\mathrm{t}}{k_{Cle2}+k_{Deg1}} + \frac{e^{-(k_{Cle2}+k_{Deg1})t}}{(k_{Cle2}+k_{Deg1})^2} - \frac{1}{(k_{Cle2}+k_{Deg1})^2}\right).$$

The S/N ratio in this case is given by dividing eq. 18 by this equation, yielding

$$\mathrm{S/N}^{route2} = \frac{k_{Pro1}\frac{k_{Txn}[DNA](k_{Cle1}+k_{Cle2})}{k_{Cle1}+k_{Cle2}+k_{Deg1}-k_{Deg2}}\left(\frac{\mathrm{t}}{k_{Deg2}}+\frac{e^{-k_{Deg2}t}}{{k_{Deg2}}^2}-\frac{\mathrm{t}}{k_{Deg1}+k_{Cle1}}-\frac{e^{-(k_{Deg1}+k_{Cle1})t}}{(k_{Deg1}+k_{Cle1})^2}-\frac{1}{{k_{Deg2}}^2}+\frac{1}{(k_{Deg1}+k_{Cle1})^2}\right)}{k_{Pro2}k_{Txn}[DNA]\left(\frac{\mathrm{t}}{k_{Cle2}+k_{Deg1}}+\frac{e^{-(k_{Cle2}+k_{Deg1})t}}{(k_{Cle2}+k_{Deg1})^2}-\frac{1}{(k_{Cle2}+k_{Deg1})^2}\right)}.$$

The S/N ratio at steady-state in this case is obtained in the same way as in case 1 as

$$\mathrm{S/N}^{route2} = \frac{k_{Pro1}}{k_{Pro2}}\frac{(k_{Cle1}+k_{Deg1}-k_{Deg2})(k_{Cle2}+k_{Deg1})(k_{Cle1}+k_{Cle2})}{k_{Deg2}(k_{Cle1}+k_{Deg1})(k_{Cle1}+k_{Cle2}+k_{Deg1}-k_{Deg2})}.$$

From eq. 8, this formulation was simplified into

$$\mathrm{S/N}^{route2} = \frac{k_{Pro1}}{k_{Pro2}}\frac{k_{Cle1}(k_{Cle2}+k_{Deg1})}{k_{Deg2}(k_{Cle1}+k_{Deg1})}.$$

Differences between our model and the previous model of Chen and Ellington

In our model (Fig. 1b), we introduced the translation route from the full-length RNA, neglected in the previous model. This route was indispensable to explain the results of mutant DelC, which produced a certain amount of protein in the absence of ligand, even though the cleaved RNA was not detected (Fig. 2g and 2h, black diamonds). We also introduced the cleaved RNA degradation process, which was required to explain the curve of the cleaved RNA (Fig. 2c and 2g). In addition, the previous model assumed that the full-length RNAs are in equilibrium of the two states, cleavage-competent and incompetent states, whereas here we assumed only one state with two different cleavage rates (k_{Cle1} and k_{Cle2}) for simplicity. This single-state assumption does not change the kinetics of any component, but only changes the assignment of parameters; k_{Cle2} in this study corresponds to multiplication of the self-cleavage rate in the previous study (k_{Cle}) with the ratio of the full-length RNA in the cleavage-competent state.

Deviation of the predicted time at which S/N ratio become constant

An easy method to determine the origin of Noise is to examine the dynamics of S/N ratio; if Noise is produced through Ligand-independent route 1 in Fig. 1c, the dynamics

of S/N ratio would rapidly become constant, whereas if Noise is produced through Ligand-independent route 2, the dynamics of S/N ratio would increase until the time of $((k_{\mathrm{Cle1}} + k_{\mathrm{Cle2}} + k_{\mathrm{Deg1}})k_{\mathrm{Deg2}})^{-\frac{1}{2}}$. The time was derived as follows.

In the case of aptazymes that produce Noise through Ligand-independent route 2, S/N ratio would increase until the cleaved RNA concentration with excess ligand becomes constant. Here, we attempted to calculate the time, τ, when the cleaved RNA concentration reaches half the final concentration after infinite time. From eq. 15, we obtained

$$\frac{[C]_{t=\tau}}{[C]_{t=\infty}} = 0.5 = \frac{\left(\frac{1-e^{-k_{Deg2}\tau}}{k_{Deg2}} - \frac{1-e^{-\alpha\tau}}{\alpha}\right)}{\left(\frac{1}{k_{Deg2}} - \frac{1}{\alpha}\right)},$$

where $\alpha = k_{Cle2} + k_{Deg1} + k_{Cle1}$.

The second-order approximation of the exponential functions gives

$\tau = ((k_{\mathrm{Cle1}} + k_{\mathrm{Cle2}} + k_{\mathrm{Deg1}})k_{\mathrm{Deg2}})^{-\frac{1}{2}}$.

Supplemental figure legends

FigureS1

Fitting of experimental data with the kinetic model.

The left and right columns show the results of Clone 1.2 (a – d) and DelC mutant (e – h), respectively. Symbols show experimental data and lines show fitting results. (a, e) The kinetics of the full-length RNA with various TPP concentrations (0 mM TPP: blue diamonds; 0.03 mM TPP: red squares; 0.1 mM TPP: green triangles; 0.3 mM TPP: purple crosses; 1 mM TPP: blue asterisks). Some of the data (0 mM, 0.03 mM, and 1 mM TPP) were the same as those in Fig. 2c and 2g. (b, f) The kinetics of the cleaved RNA with various TPP concentrations. The symbols are the same as described above. These full-length and cleaved RNA data were fitted with eq. 13 and 15 to estimate k_{Deg1}, k_{Deg2} and α, which represents $k_{Cle2} + k_{Deg1} + \frac{k_{Cle1}[L_{Total}]}{K_d + [L_{Total}]}$. (c, g) The values of α were further plotted to the ligand concentration and fitted with eq. 14 to estimate k_{Cle2}, k_{Cle1}, and K_{d}. (d, h) The ratio of deviation of protein concentration to the total full-length RNA concentration (d[Protein]/dt/[$\mathrm{F_{Total}}$]) was plotted against that of the cleaved RNA concentration to the total full-length RNA concentration ([C]/[$\mathrm{F_{Total}}$]) and fitted with eq. 17 to estimate k_{Pro1} and k_{Pro2}. The experimental values of d[Protein]/dt were obtained

from the slope of protein concentrations with ligand concentrations (0 – 0.1 mM) every 10 min. The values of [C] and [F_{Total}] were obtained from the simulation using eq. 13 and 15 and the parameters in Table 1 (see Materials and Methods for more information regarding parameter estimation).

Figure S2

Comparison of GFP protein concentration measured by radioisotope incorporation assay (triangles) and that calculated from the GFP fluorescence using a conversion factor (line). The method of radioisotope incorporation assay is described in the Materials and Methods. The conversion factor (1/165) was determined to minimize the difference between the protein concentrations measured by the two methods. Here, we assumed a lag time of 10 min for GFP protein to produce fluorescence because GFP is known to take a certain time to fold into the active state that emits fluorescence.

Figure S3

Effects of mutations that lengthen the stem-containing SD sequence on the S/N ratio. Mutations (M1–M3) that are presumed to lengthen the stem of the SD sequence were introduced into Clone 1.2 or DelC aptazyme. (a) Plausible structure around the stem

of each mutant, where the mutations are highlighted in yellow and the SD sequence is shown in red. (b) The S/N ratio at 100 min of the mutants of Clone 1.2 and DelC.

Figure S4

Kinetics of the RNAs and the S/N ratio of theophylline responsive aptazyme developed by Ogawa and Maeda (Ogawa et al. 2007). The GFP gene was attached to the aptazyme and the fluorescence was measured by the same was as the TPP responsive aptazymes. (a) S/N ratio. The S/N ratio was defined as the ratio of GFP fluorescence at 2 mM theophylline to that at 0 mM theophylline. The kinetics of the full-length (b) and the cleaved RNA (c) were measured at 0 mM (black diamonds) or 2 mM theophylline (gray circles). Fitting results are indicated by lines. Note that we used a shortened version of the GFP gene (356 nt shorter) for measurement of the full-length and cleaved RNA because the size difference between full-length and cleaved RNA of original construct is too small to allow them to be distinguished.

Figure S1

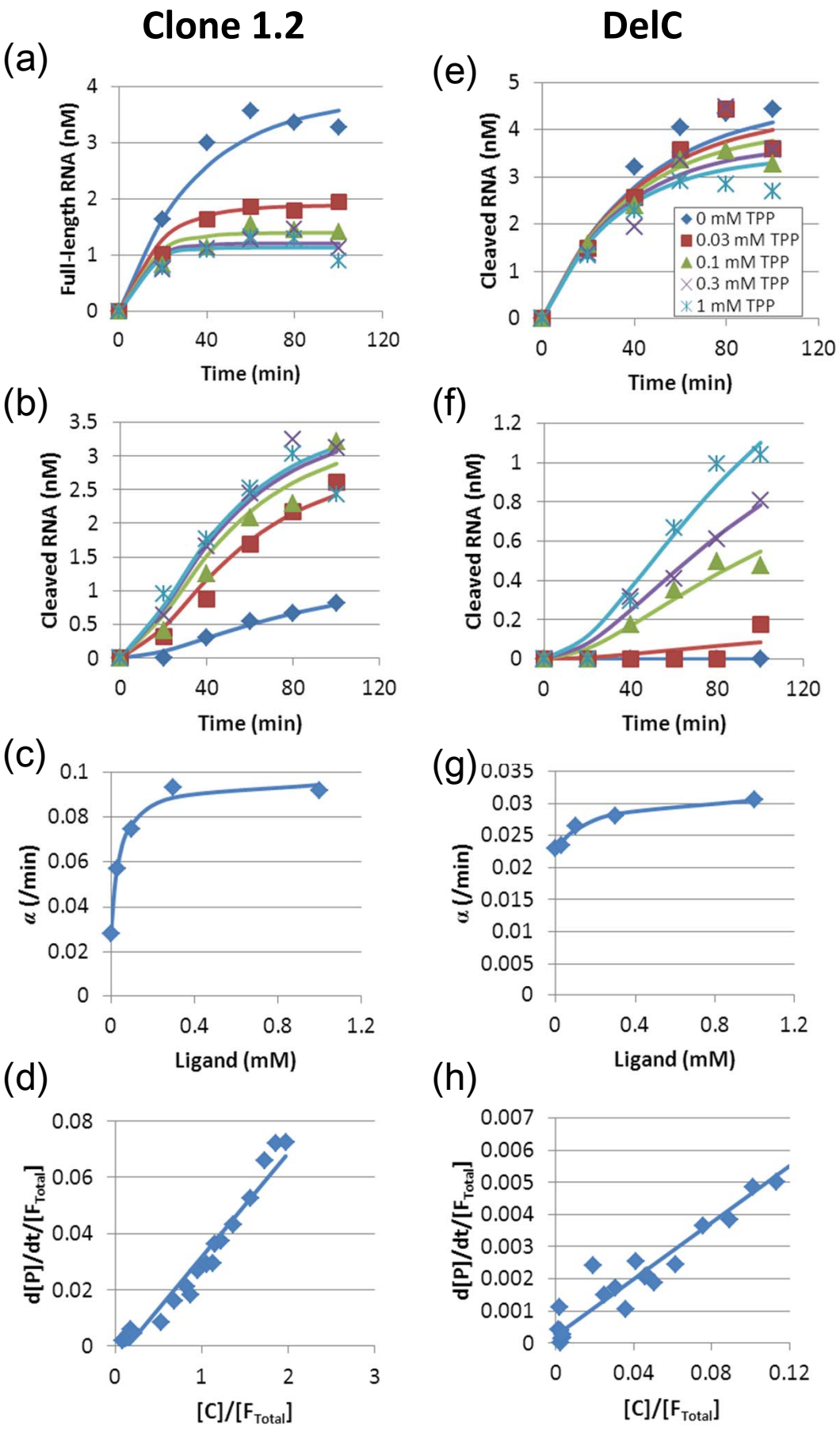
Clone 1.2
DelC
(a)
(b)
(c)
(d)
(e)
(f)
(g)
(h)
Full-length RNA (nM)
Cleaved RNA (nM)
Time (min)
0 mM TPP
0.03 mM TPP
0.1 mM TPP
0.3 mM TPP
1 mM TPP
α (/min)
Ligand (mM)
d[P]/dt/[F_Total]
[C]/[F_Total]

Figure S2

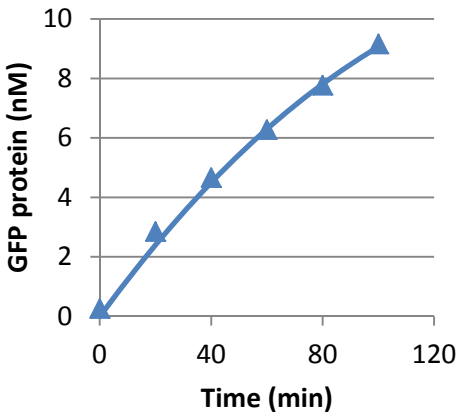

Figure S3

(a)

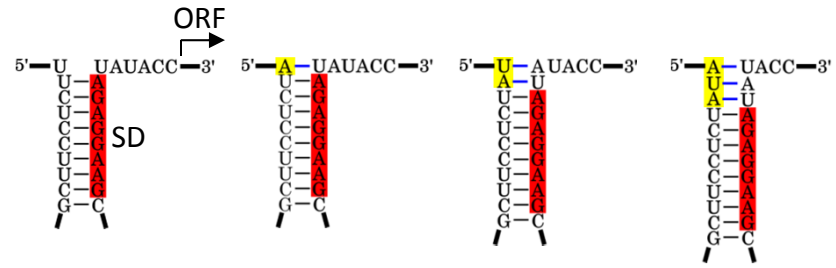

No mutation M1 M2 M3

(b)

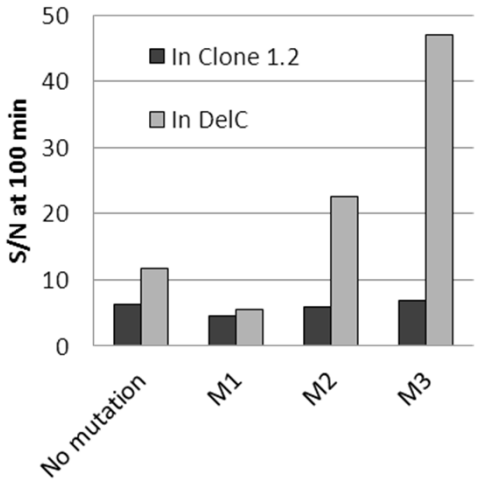

Figure S4

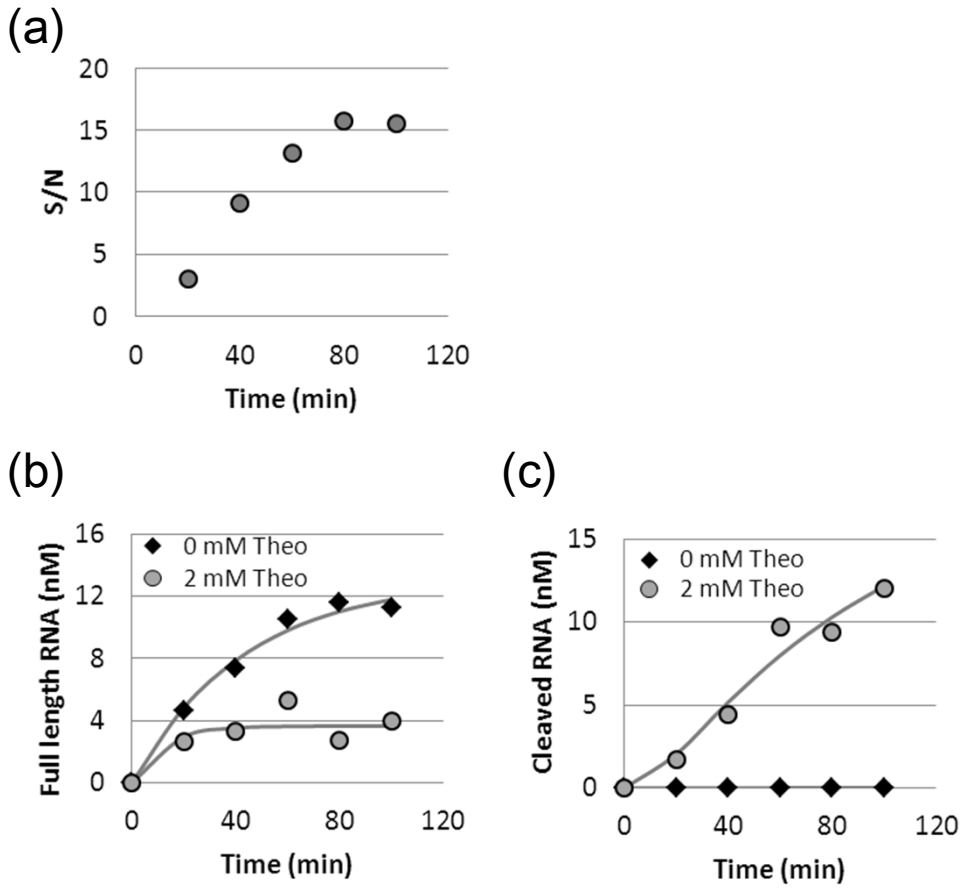
(a)
S/N
20
15
10
5
0
0
40
80
120
Time (min)
(b)
Full length RNA (nM)
16
12
8
4
0
0 mM Theo
2 mM Theo
0
40
80
120
Time (min)
(c)
Cleaved RNA (nM)
15
10
5
0
0 mM Theo
2 mM Theo
0
40
80
120
Time (min)